CONSTRUCTIONS

Mechanical and Durability Properties of Geopolymer Concrete Made from Bamboo Leaf Ash and Rice Husk Ash

Joseph Oluwabukunmi Ishola, B. I. O. Dahunsi

Department of Civil Engineering, University of Ibadan, Ibadan, Nigeria

Published November 2026

Abstract

This study investigated the mechanical and durability properties of concrete made with bamboo leaf ash (BLA) and rice husk ash (RHA) as the only solid precursors, activated with sodium hydroxide and sodium silicate. X-ray fluorescence (XRF) analysis showed both ashes to be highly siliceous (SiO_2 of 90.97% in RHA and 83.36% in BLA) but very low in alumina (0.38% and 1.78%). Five BLA:RHA ratios (100:0, 75:25, 50:50, 25:75 and 0:100 by mass) were compared with a grade C25 control concrete. Slump, density, compressive strength (7, 14 and 28 days), splitting tensile and flexural strength (56 days), and water absorption and depth of water penetration (28 and 56 days) were determined. Workability decreased as RHA content increased, from a slump of 110 mm for the control to 35 mm for the RHA-only mix. The 28-day compressive strength of the alkali-activated mixes ranged from 15.80 to 24.62 N/mm^2, against 26.33 N/mm^2 for the control. The 50:50 blend gave the highest strength among the alkali-activated mixes, reaching 93.5% of the control strength and not differing significantly from it (Tukey, $p = 0.45$). It also gave the highest 56-day flexural strength of the alkali-activated mixes (3.47 N/mm^2, 74.9% of the control). Water absorption rose from 1.24% for the control to between 2.17% and 7.93% for the alkali-activated mixes, and penetration depth followed the same trend. A 50:50 blend gave the best overall balance of strength, workability and water resistance among the mixes tested, indicating that these two agricultural wastes can be combined as the solid precursor of laboratory-scale alkali-activated concrete of moderate strength. The findings rest on small specimen numbers and do not establish long-term durability or structural suitability; they should be confirmed in larger test programmes.

Keywords: alkali activation; bamboo leaf ash; durability; alkali-activated concrete; rice husk ash

1 Introduction

Concrete is the most widely used construction material, but the production of Portland cement is energy-intensive and a major source of anthropogenic carbon dioxide emissions [1]. This has driven research into alternative binders. Geopolymers, made by alkali activation of aluminosilicate materials such as fly ash and metakaolin, are one low-carbon option [2–5], and low-calcium fly ash geopolymer concrete can combine good compressive strength, low drying shrinkage and good sulfate resistance [6]. The carbon benefit, however, depends on system boundaries, activators, curing regime and transport distances, so it cannot be assumed universally [7].

Under alkaline conditions, reactive silicon and aluminium species dissolve and recondense into binding gels, which, depending on the calcium content of the precursor, are N-A-S-H, C-(A)-S-H or a mixture of both [8, 9]. Activator concentration and curing temperature strongly influence dissolution and strength development [10, 11].

Agricultural residues are attractive precursors where they are abundant and are often disposed of by open burning. Rice husk ash (RHA) is rich in amorphous silica when burned under controlled conditions, but its residual carbon, fineness and reactivity depend on the husk source and the combustion method, and its porous, high-surface-area particles increase water demand [12]. Bamboo leaf ash (BLA) is also silica-rich and pozzolanic after calcination [13], and has been used in concrete and in geopolymer concrete cured at ambient temperature [14, 15]. RHA has mostly been studied in geopolymers as a silica supplement to alumina-rich precursors such as fly ash [16–18], and its effects on strength and durability have been reviewed [19–21].

Silica content alone does not make a good geopolymer precursor, because geopolymerisation also requires reactive alumina [3], and both ashes contain little of it. To the authors' knowledge, the use of BLA and RHA together as the only solid precursors in concrete, and the effect of their relative proportions on mechanical and durability performance, has not been reported.

This paper reports an experimental study of concrete in which BLA and RHA were the only solid precursors, activated with sodium hydroxide and sodium silicate. Five BLA:RHA ratios were compared with a grade C25 control concrete. Workability, density, compressive strength (7, 14 and 28 days), splitting tensile and flexural strength (56 days), water absorption and depth of water penetration (28 and 56 days) were measured to identify the blend giving the best overall performance. The oxide composition of both ashes was determined by X-ray fluorescence (XRF). The term alkali-activated concrete is nevertheless used because XRF gives only the bulk chemistry of the ashes, and the mineralogical and microstructural evidence needed to confirm a geopolymer binder was not available.

2 Materials and methods

2.1 Materials

Bamboo leaves and rice husk were collected from Hybrid Feed Ltd, KM 10, Old Lagos Road, opposite Lister Flour Mills, Podo, Ibadan, Oyo State, Nigeria, and from the Baptist Church, University of Ibadan, cleaned of soil and foreign matter, and air-dried. Each material was burned separately in a furnace under controlled conditions, the bamboo leaves at 600 °C and the rice husk at 750 °C, each for 3 hours, to obtain ashes rich in amorphous silica [12, 13]. The ashes were cooled, ground, sieved through a 75 μm sieve and stored in labelled airtight containers. About 25 kg of bamboo leaves and 15 kg of rice husk were needed to produce 1 kg of ash. The oxide composition and loss on ignition (LOI) of the two ashes were determined by energy-dispersive X-ray fluorescence (EDXRF) at Spectrum Analytical Services, Kaduna, Nigeria (report SAS/GEN/2026/09/010); the results are presented in Section III-A. The particle size, specific surface area and mineralogy of the ashes were not determined.

The alkaline activator was a mixture of sodium hydroxide (NaOH) solution and sodium silicate (Na_2SiO_3) solution. The 10 M NaOH solution was prepared by dissolving pellets in water, allowed to cool and rest for about 24 h, and then blended with the sodium silicate solution at a NaOH:Na_2SiO_3 mass ratio of 1:2.5. The same activator formulation was used for all alkali-activated mixes. The fine aggregate was clean natural sand, tested for particle size distribution, fineness modulus, specific gravity, bulk density and water absorption. The coarse aggregate was crushed stone with a nominal maximum size of 20 mm. Potable water was used throughout. No Portland cement, metakaolin, fly ash or slag was used in the alkali-activated mixes.

2.2 Mix proportions

Five alkali-activated mixes (M1–M5) were produced in which the ash precursor, by mass, was varied from 100% BLA to 100% RHA (Table 1). These percentages refer to the ash precursor only, not to the total concrete mass. The total precursor content, aggregate proportions, activator-to-binder ratio, Na_2SiO_3:NaOH ratio and NaOH molarity were held constant across the five mixes. The mix quantities were established from trial batches in which workability, cohesion and compaction were assessed. Each batch contained 8.21 kg of ash precursor (BLA and RHA in the proportions of Table 1), 32.82 kg of fine aggregate, 65.65 kg of coarse aggregate, 2.34 kg of NaOH solution and 5.86 kg of Na_2SiO_3 solution, which gives an activator-to-binder mass ratio of about 1.0 and a NaOH:Na_2SiO_3 ratio of 1:2.5. The control was a conventional grade C25 concrete made with CEM II/B-L 42.5N cement, designed by the DOE method with a water–cement ratio of 0.5.

Table 1. Ash precursor proportions of the mixes.

Mix	BLA (%)	RHA (%)	BLA:RHA
Control (C25)	–	–	–
M1	100	0	100:0
M2	75	25	75:25
M3	50	50	50:50
M4	25	75	25:75
M5	0	100	0:100

2.3 Specimen production and curing

The BLA and RHA were weighed and dry-mixed until uniform, the fine and coarse aggregates were mixed separately, and the two were then combined. The activator was added slowly and mixing continued until the concrete was homogeneous. Workability was assessed by the slump test. The concrete was placed in clean, lightly oiled moulds in layers and compacted with a tamping rod in the same way for every batch. Specimens were covered after casting to prevent evaporation and demoulded after 24 hours. A single curing regime was used for all mixes: heat curing at 60 °C for 24 hours, followed by curing under ambient laboratory conditions at about 27 °C until testing. Because one regime was used, the effect of curing was not investigated.

Concrete was cast into 150 mm cubes for density, compressive strength (three cubes per mix at 7, 14 and 28 days), water absorption and water penetration (one cube per mix at 28 and 56 days); 100 mm × 200 mm cylinders for splitting tensile strength (two per mix at 56 days); and 100 × 100 × 400 mm beams for flexural strength (two per mix at 56 days).

2.4 Testing

Compressive strength was determined in a universal testing machine (Figure 1a) at a loading rate of 15 kN/s, in accordance with BS EN 12390-3 [22] as

$$f_c = \frac{P}{A} \tag{1}$$

where P is the maximum load at failure and A is the loaded area. Splitting tensile strength was determined in accordance with BS EN 12390-6 [23] as

$$f_t = \frac{2P}{\pi DL} \quad (2)$$

where D and L are the cylinder diameter and length. Flexural strength was calculated with the centre-point loading expression as

$$f_b = \frac{3PL}{2bd^2} \quad (3)$$

where L is the span, taken as 100 mm as recorded on the laboratory data sheet, and b and d are the beam width and depth, both 100 mm (Figure 1b). Water absorption was calculated as

$$A_w(\%) = \frac{M_2 - M_1}{M_1} \times 100 \quad (4)$$

where M_1 and M_2 are the oven-dry and saturated surface-dry masses of the cube. The cubes were dried to constant mass at 100 ± 5 °C and immersed in water for 24 hours, following ASTM C642 [24]. The depth of water penetration was measured as an indicator of permeability by applying water at 500 ± 50 kPa (5 bar) for 72 ± 2 hours (3 days) under constant pressure, following BS EN 12390-8 [25], in which the specimen is split after the test and the maximum depth of the wetted zone is measured. Results are reported as the mean and standard deviation (SD) of the specimens tested. A one-way analysis of variance (ANOVA) with a Tukey post-hoc test at the 5% significance level was applied to the 28-day compressive strengths. No inferential statistics were applied to the tensile, flexural and durability results because only one or two specimens were tested per mix.

3 Results and discussion

3.1 Chemical composition of the ashes

The oxide compositions of the RHA and BLA are given in Table 2. Both ashes are highly siliceous: SiO_2 is 90.97% in the RHA and 83.36% in the BLA, and no other oxide exceeds 1.75% in the RHA or 3.50% in the BLA. The combined SiO_2 + Al_2O_3 + Fe_2O_3 contents (93.10% and 88.64%) exceed the 70% minimum of ASTM C618 for Class N pozzolans, and the SO_3 contents and LOI are within its limits of 4% and 10% [26]. This is a chemical comparison only: XRF does not distinguish amorphous from crystalline silica and so does not establish reactivity [27], and the reactivity of RHA silica depends on its burning temperature and duration [31].

Table 2. Chemical composition of the ashes determined by XRF (mass %).

Constituent	RHA	BLA
SiO_2	90.97	83.36
Al_2O_3	0.38	1.78
Fe_2O_3	1.75	3.50
CaO	0.71	2.45
MgO	ND	1.24
Na_2O	0.56	1.48
K_2O	1.71	3.06
SO_3	0.02	0.38

Constituent	RHA	BLA
TiO_2	0.05	0.20
MnO	0.13	0.14
P_2O_5	1.54	0.45
LOI	2.14	2.80
$SiO_2 + Al_2O_3 + Fe_2O_3$	93.10	88.64
$Na_2O + K_2O$	2.27	4.54
SiO_2/Al_2O_3 (molar)	406.2	79.5

ND = not detected. Derived values calculated from the reported data (molar masses SiO_2 = 60.08 g/mol, Al_2O_3 = 101.96 g/mol).

The critical deficiency is alumina, at only 0.38% in the RHA and 1.78% in the BLA. The resulting SiO_2/Al_2O_3 molar ratios (about 406 and 80, i.e. Si/Al of about 203 and 40) are far above the Si/Al range of roughly 1 to 3 on which aluminosilicate geopolymer frameworks are based and within which composition strongly controls microstructure and strength [3, 28, 29]. Both ashes are therefore better described as reactive-silica sources than as balanced aluminosilicate precursors, which supports the use of the term alkali-activated concrete. The BLA is the more favourable of the two, containing about 4.7 times as much Al_2O_3, 3.5 times as much CaO and twice as much $Na_2O + K_2O$ as the RHA. CaO is below 2.5% in both ashes, so with 10 M NaOH any contribution from calcium-bearing C-(A)-S-H gel is likely to be small [30]. The appreciable alkali content combined with very little alumina also suggests a possible susceptibility to efflorescence [32], which was not assessed. Because the mixes differ only in ash proportions, the precursor composition changes linearly with the BLA:RHA ratio: the Al_2O_3 content falls from 1.78% (100:0) to 1.43%, 1.08%, 0.73% and 0.38% (0:100), and the SiO_2/Al_2O_3 molar ratio rises from about 80 to 101, 137, 207 and 406.

3.2 Fine aggregate

The sand had a fineness modulus of 2.47, a specific gravity of 2.61, a bulk density of 1,648 kg/m^3, a water absorption of 0.78% and 0.31% passing the 0.075 mm sieve. The percentage passing the 0.60 mm sieve (47.1%) places it in Zone 2 of BS 882 [33]. It is a clean, medium-grade sand suitable for concrete and unlikely to increase water demand.

3.3 Workability and density

Workability fell steadily as the RHA proportion increased (Table 3). The slump of the control was 110 mm, compared with 94 mm for the BLA-only mix and only 35 mm for the RHA-only mix, a reduction of 68%. RHA particles are reported to be angular, porous and of high specific surface area [12], which may cause them to adsorb mixing liquid and leave less free liquid to lubricate the mix, and the alkaline activator may also make the pastes more viscous than cement pastes. These explanations were not tested here because the particle properties of the ashes were not measured. The 100:0 and 75:25 mixes remained in the medium-workability range, the 50:50 and 25:75 mixes were of low workability, and the 0:100 mix would need extra liquid, a superplasticiser or a different activator-to-binder ratio to be placed easily.

Table 3. Slump and 28-day density of the concrete mixes.

Mix (BLA:RHA)	Slump (mm)	Slump reduction (%)	Density (kg/m³)
Control	110	–	2,443
100:0	94	14.5	2,383
75:25	75	31.8	2,370
50:50	63	42.7	2,401
25:75	58	47.3	2,375
0:100	35	68.2	2,363

The 28-day densities of the alkali-activated mixes (2,363–2,401 kg/m^3) were 1.7–3.3% lower than that of the control but all fall within the normal-weight range (2,200–2,600 kg/m^3). Densities at 7 and 14 days were similar, apart from a few cubes that were appreciably lighter (e.g. 2,103 kg/m^3 for one 75:25 cube at 7 days). These low values may indicate incomplete compaction or entrapped air, which could have contributed to the scatter in strength at those ages.

3.4 Compressive strength

Compressive strengths are given in Table 4 and Figure 2. All mixes gained strength between 7 and 28 days. The control reached 26.33 N/mm^2, above the 25 N/mm^2 target for grade C25. The control, 100:0, 75:25 and 50:50 mixes gained 49–55% of their 7-day strength by 28 days, and had reached about 65% of their 28-day strength at 7 days. The 25:75 and 0:100 mixes gained only 24% and 18%, and had reached 80% and 85% of their 28-day strength at 7 days. Strength development of the RHA-rich binders therefore levelled off early, which may indicate that their reaction was limited after the early age, which is consistent with the very low alumina content of these precursors (Section III-A), although this could not be verified without mineralogical or microstructural tests.

Table 4. Compressive strength (N/mm^2, mean ± SD, n = 3).

Mix (BLA:RHA)	7 days	14 days	28 days
Control	17.70 ± 1.39	22.31 ± 0.92	26.33 ± 2.25
100:0	14.25 ± 0.36	18.48 ± 0.51	22.00 ± 0.31
75:25	14.90 ± 0.28	20.57 ± 0.56	22.70 ± 0.84
50:50	15.88 ± 0.44	21.30 ± 0.33	24.62 ± 0.74
25:75	14.98 ± 0.11	17.71 ± 0.28	18.63 ± 0.64
0:100	13.39 ± 0.28	14.42 ± 0.36	15.80 ± 0.69

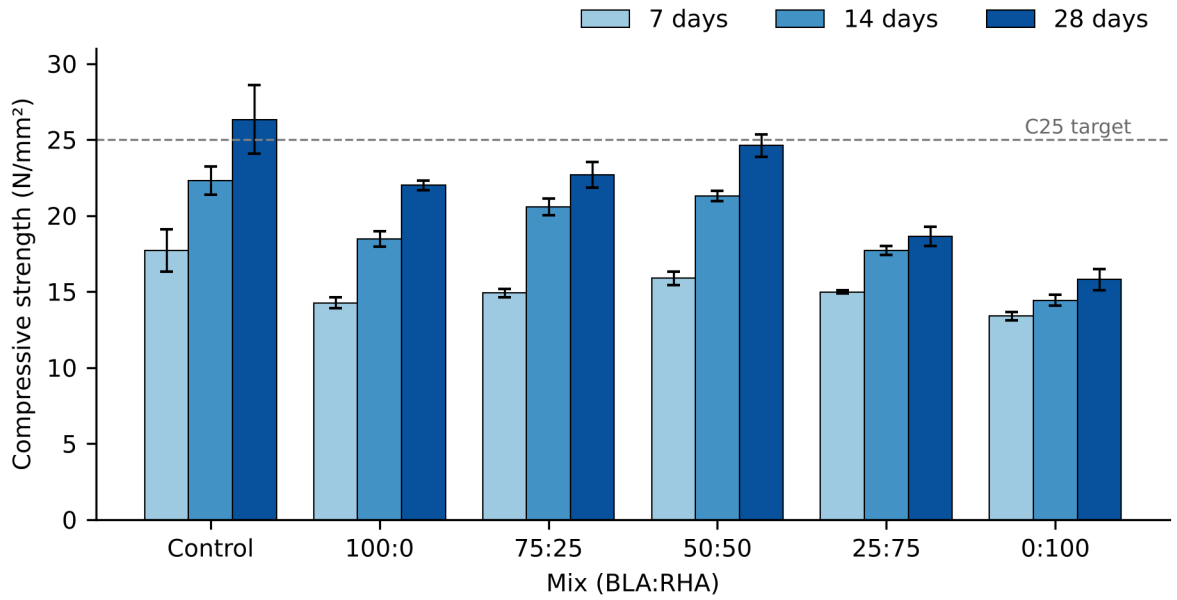


Figure 2. Compressive strength of the mixes at 7, 14 and 28 days (error bars show ±1 SD).

Among the alkali-activated mixes, the 50:50 blend gave the highest mean strength at every age, reaching 24.62 N/mm^2 at 28 days (93.5% of the control). The 100:0 and 75:25 mixes gave 22.00 and 22.70 N/mm^2 (83.5% and 86.2%), while strength fell sharply when RHA was the majority component, to 18.63 N/mm^2 for 25:75 and 15.80 N/mm^2 for 0:100 (70.7% and 60.0%) (Figure 3a). Strength therefore rose as RHA replaced BLA up to equal proportions and then fell. The XRF results (Section III-A) do not support an explanation of the peak at 50:50 based on bulk chemistry alone: because the composition of a blend lies between those of the two ashes, the 50:50 precursor contains less Al_2O_3 (1.08%), CaO and alkali than the 100:0 and 75:25 precursors. The small advantage of the 50:50 mix, which was not statistically significant relative to the 75:25 mix, may instead reflect differences in the amorphous silica content, fineness and particle packing of the two ashes, which were not measured. By contrast, the sharp loss of strength in the RHA-rich mixes is consistent with their very low alumina contents (0.73% and 0.38% in the 25:75 and 0:100 precursors) and high SiO_2/Al_2O_3 molar ratios (about 207 and 406), conditions under which little aluminosilicate cross-linking would be expected [28, 29]. The poor performance of the RHA-rich mixes is also consistent with their low workability: stiff mixes may be harder to compact and leave more voids, and the water absorption results in Section III-F are consistent with a more porous matrix, although porosity was not measured.

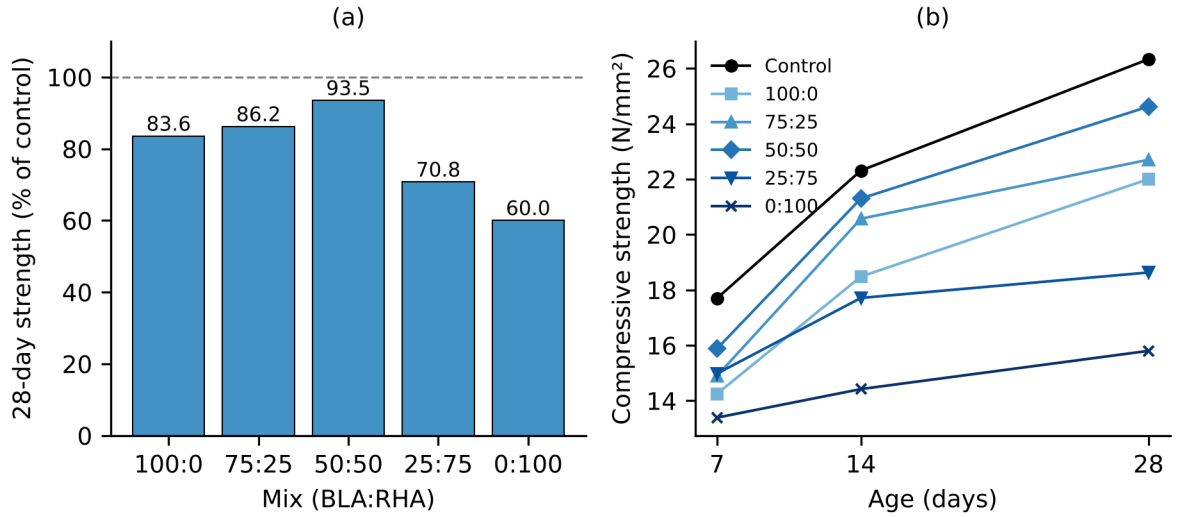


Figure 3. (a) 28-day compressive strength relative to the control; (b) strength development with age.

A one-way ANOVA of the 28-day results showed that the BLA:RHA ratio had a significant effect on strength (F = 37.1, p < 0.001). The Tukey test showed that the 50:50 mix was not significantly different from the control (p = 0.45), whereas the control differed significantly from the other four alkali-activated mixes. The 100:0 and 75:25 mixes were not significantly different from each other (p = 0.97), nor were the 25:75 and 0:100 mixes (p = 0.07). The 50:50 and 75:25 mixes were also not significantly different from each other (p = 0.33), so the ranking of the 50:50 mix above the 75:25 mix is not statistically established. With three specimens per mix, these tests have limited power.

Only the control exceeded the 25 N/mm^2 target at 28 days. The 50:50 mix (24.62 N/mm^2) came within 1.5% of it, which is within the scatter of the test, but strictly it did not reach grade C25. On mean 28-day strength alone, the 100:0 and 75:25 mixes would suit a lower grade such as C20, and the 25:75 and 0:100 mixes non-structural uses only.

3.5 Splitting tensile and flexural strength

Splitting tensile and flexural strengths at 56 days are given in Table 5. The control had the highest values in both tests. Among the alkali-activated mixes, the 50:50 and 25:75 mixes gave the highest tensile strength (81% and 84% of the control) and the 100:0 mix the lowest (57%). Unlike compressive strength, the tensile strength of the 25:75 mix matched that of the 50:50 mix, but with two specimens per mix this is an observation and not a firm trend, and no explanation was tested. For flexure, the control beams gave a mean of 4.64 N/mm^2, and the 50:50 mix again gave the highest flexural strength of the alkali-activated mixes (3.47 N/mm^2, 74.9% of the control), followed by 75:25 (3.16 N/mm^2, 68.2%), while the 100:0, 25:75 and 0:100 mixes gave 2.73–2.87 N/mm^2 (59–62%). The alkali-activated beams were also lighter than the control beams (7.93–9.31 kg against 9.66–9.94 kg), which is consistent with their lower density.

Table 5. Splitting tensile and flexural strength at 56 days (n = 2).

Mix (BLA:RHA)	Tensile (N/mm²)	% of control	Flexural (N/mm²)	% of control
Control	0.69	100	4.64	100
100:0	0.39	56.5	2.76	59.5

Mix (BLA:RHA)	Tensile (N/mm²)	% of control	Flexural (N/mm²)	% of control
75:25	0.43	62.3	3.16	68.2
50:50	0.56	81.2	3.47	74.9
25:75	0.58	84.1	2.73	58.9
0:100	0.46	66.7	2.87	61.8

Only two specimens per mix were tested, and the absolute magnitudes in Table 5 should be treated with caution: relative to the 28-day compressive strength, the control tensile strength is low (about 3%) and its flexural strength relatively high (about 18%) compared with values usually expected for concrete. The flexural values were calculated with the centre-point expression using the 100 mm span, beam width and depth recorded on the laboratory data sheet; because flexural strength is proportional to the span, the absolute values would change in proportion if the actual distance between the supports differed from the recorded value. The tensile values are consistent with the recorded failure loads and cylinder dimensions but still require verification against the laboratory records. The results are therefore interpreted comparatively, as ratios to the control, and are indicative.

3.6 Durability

Water absorption increased consistently with RHA content (Table 6). At 28 days it rose from 1.24% for the control to 2.17% for the BLA-only mix and 7.93% for the RHA-only mix, more than six times the control. Relative to the control, the 100:0 mix absorbed less than twice as much water, the 75:25 and 50:50 mixes about three times as much, and the 25:75 and 0:100 mixes more than five times as much. The 56-day absorption was almost the same as at 28 days for most mixes; the small differences for the control (1.24 to 1.48%) and the 0:100 mix (7.93 to 7.40%) should not be over-interpreted because only one specimen per mix was tested. The high absorption of the RHA-rich mixes is in line with their low workability and strength and may reflect a more porous, less well compacted matrix, although pore structure was not measured. The absorption ranking also follows the decrease in the alumina content of the precursor (Section III-A), but with single specimens this agreement does not establish a causal link. These are experimental observations from single specimens and do not establish long-term durability.

Table 6. Water absorption and depth of water penetration.

Mix (BLA:RHA)	Absorption 28 d (%)	Absorption 56 d (%)	Depth 28 d (mm)	Depth 56 d (mm)
Control	1.24	1.48	2.8	3.0
100:0	2.17	2.39	4.0	4.7
75:25	3.59	3.80	5.5	6.0
50:50	3.77	3.77	6.8	7.0
25:75	6.40	6.41	8.7	9.0
0:100	7.93	7.40	9.6	10.2

The depth of water penetration followed the same pattern. At 28 days it increased from 2.8 mm for the control to 9.6 mm for the 0:100 mix, and the correlation between 28-day absorption and penetration depth was very strong (r = 0.98), which is consistent with both tests reflecting the

volume and connectivity of the pores (this correlation rests on six single-specimen values). Penetration in the alkali-activated mixes was 1.4 to 3.4 times that of the control, although all depths were small in absolute terms (at most 10.2 mm). Penetration depth increased slightly between 28 and 56 days for every mix (by about 3–18%), the opposite of the trend expected if continued reaction refines the pores. Because different specimens were tested at each age without replication, this may reflect specimen variation or test conditions, and no mechanism can be inferred from these data.

3.7 Overall performance

Across the properties tested, the 50:50 BLA:RHA mix gave the best overall balance of properties among the alkali-activated mixes: it gave the highest compressive and flexural strength of those mixes, near-best tensile strength, and moderate workability and absorption. It was not the best mix in every property: the BLA-only mix had the highest slump and lowest absorption, and the 25:75 mix a marginally higher tensile strength. Increasing the RHA content beyond this level reduced workability, strength and durability. The BLA-only mix had the best workability and durability of the alkali-activated mixes but a lower strength than the blend.

4 Conclusion

Concrete made with BLA and RHA as the only solid precursors reached 28-day compressive strengths of 15.80–24.62 N/mm^2, against 26.33 N/mm^2 for a grade C25 control. A 50:50 blend gave the best overall balance of strength, workability and water resistance among the mixes investigated, although not the best in every property, with a compressive strength not significantly different from the control or from the 75:25 mix, whereas RHA-rich mixes (25:75 and 0:100) were stiff, slow to gain strength and porous, and are not recommended for structural use without modification. The results show that these two agricultural wastes can be combined as the solid precursor of laboratory-scale alkali-activated concrete of moderate strength; they do not establish long-term durability or structural suitability.

The findings are limited by small specimen numbers (three cubes, two cylinders or beams, and one absorption specimen per mix and age), a single activator ratio and curing method, and the absence of mineralogical and microstructural characterisation. The tensile results and the span used in the flexural test also require verification against the laboratory records, and the short-term tests do not establish long-term durability. XRF analysis showed that both ashes are highly siliceous but very low in alumina (0.38% in RHA and 1.78% in BLA), so the binder is best regarded as an alkali-activated ash-based system unless microstructural analyses (FTIR, SEM/EDS) show otherwise. Further work should optimise the activator-to-binder ratio and NaOH concentration of the 50:50 blend to reach 25 N/mm^2 or more, use superplasticiser or additional liquid in RHA-rich mixes, compare ambient and heat curing, examine the addition of a small proportion of an alumina-rich precursor, repeat the tensile, flexural and permeability tests with verified loads and more specimens, and examine acid and sulfate resistance, chloride penetration, shrinkage and elevated-temperature performance.

Acknowledgments

The authors acknowledge the academic and technical staff of the Department of Civil Engineering, University of Ibadan, for their support during this work.

References

[1] Andrew RM. Global CO_2 emissions from cement production. *Earth Syst Sci Data*. 2018;10(1):195–217. https://doi.org/10.5194/essd-10-195-2018

[2] Davidovits J. Geopolymers and geopolymeric materials. *J Therm Anal*. 1989;35(2):429–441. https://doi.org/10.1007/BF01904446

[3] Duxson P, Fernández-Jiménez A, Provis JL, Lukey GC, Palomo A, van Deventer JSJ. Geopolymer technology: the current state of the art. *J Mater Sci*. 2007;42(9):2917–2933. https://doi.org/10.1007/s10853-006-0637-z

[4] Duxson P, Provis JL, Lukey GC, van Deventer JSJ. The role of inorganic polymer technology in the development of 'green concrete'. *Cem Concr Res*. 2007;37(12):1590–1597. https://doi.org/10.1016/j.cemconres.2007.08.018

[5] Turner LK, Collins FG. Carbon dioxide equivalent (CO_2-e) emissions: a comparison between geopolymer and OPC cement concrete. *Constr Build Mater*. 2013;43:125–130. https://doi.org/10.1016/j.conbuildmat.2013.01.023

[6] Hardjito D, Rangan BV. *Development and properties of low-calcium fly ash-based geopolymer concrete*. Research Report GC 1. Perth: Faculty of Engineering, Curtin University of Technology; 2005.

[7] Shobeiri V, Bennett B, Xie T, Visintin P. A comprehensive assessment of the global warming potential of geopolymer concrete. *J Clean Prod*. 2021;297:126669.

[8] Provis JL. Alkali-activated materials. *Cem Concr Res*. 2018;114:40–48. https://doi.org/10.1016/j.cemconres.2017.02.009

[9] Luukkonen T, Abdollahnejad Z, Yliniemi J, Kinnunen P, Illikainen M. One-part alkali-activated materials: a review. *Cem Concr Res*. 2018;103:21–34. https://doi.org/10.1016/j.cemconres.2017.10.001

[10] Rattanasak U, Chindaprasirt P. Influence of NaOH solution on the synthesis of fly ash geopolymer. *Miner Eng*. 2009;22(12):1073–1078. https://doi.org/10.1016/j.mineng.2009.03.022

[11] Oyebisi S, Ede A, Olutoge F, Ofuyatan O, Oluwafemi J. Influence of alkali concentrations on the mechanical properties of geopolymer concrete. *Int J Civ Eng Technol*. 2018;9(8):725–733.

[12] Habeeb GA, Mahmud HB. Study on properties of rice husk ash and its use as cement replacement material. *Mater Res*. 2010;13(2):185–190. https://doi.org/10.1590/S1516-14392010000200011

[13] Villar-Cociña E, Valencia-Morales E, Santos SF, Savastano H, Frías M. Pozzolanic behavior of bamboo leaf ash: characterization and determination of the kinetic parameters. *Cem Concr Compos*. 2011;33(1):68–73. https://doi.org/10.1016/j.cemconcomp.2010.09.003

[14] Said H, Silvester A, Mwero JN. Effect of bamboo leaf ash on the properties of geopolymer concrete at ambient curing temperature. *East Afr J Eng*. 2023;6(1):88–103. https://doi.org/10.37284/eaje.6.1.1210

[15] Nduka DO, Olawuyi BJ, Ajao AM, Okoye VC, Okigbo OM. Mechanical and durability property dimensions of sustainable bamboo leaf ash in high-performance concrete. *Clean Eng Technol*. 2022;11. https://doi.org/10.1016/j.clet.2022.100583

[16] Detphan S, Chindaprasirt P. Preparation of fly ash and rice husk ash geopolymer. *Int J Miner Metall Mater*. 2009;16(6):720–726.

[17] Songpiriyakij S, Kubprasit T, Jaturapitakkul C, Chindaprasirt P. Compressive strength and degree of reaction of biomass- and fly ash-based geopolymer. *Constr Build Mater*. 2010;24(3):236–240.

[18] Nazari A, Bagheri A, Riahi S. Properties of geopolymer with seeded fly ash and rice husk bark ash. *Mater Sci Eng A*. 2011;528(24):7395–7401. https://doi.org/10.1016/j.msea.2011.06.027

[19] Abbass M, Singh G. Durability of rice husk ash and basalt fibre based sustainable geopolymer concrete in rigid pavements. *Mater Today Proc*. 2022;61:558–570. https://doi.org/10.1016/j.matpr.2022.02.196

[20] Zeyad AM, Bayraktar OY, Tayeh BA, Öz A, Özkan İGM, Kaplan G. Impact of rice husk ash on physico-mechanical, durability and microstructural features of rubberized lightweight geopolymer composite. *Constr Build Mater*. 2024;427. https://doi.org/10.1016/j.conbuildmat.2024.136265

[21] Hamada HM, Al-Attar A, Beddu S, Askar MK, Yousif ST, Majdi A. Impact of rice husk ash on geopolymer concrete: a literature review and future directions. *Case Stud Constr Mater*. 2025;22. https://doi.org/10.1016/j.cscm.2025.e04476

[22] British Standards Institution. *BS EN 12390-3:2019 Testing hardened concrete—Part 3: compressive strength of test specimens*. London: BSI; 2019.

[23] British Standards Institution. *BS EN 12390-6:2023 Testing hardened concrete—Part 6: tensile splitting strength of test specimens*. London: BSI; 2023.

[24] ASTM International. *ASTM C642-21 Standard test method for density, absorption, and voids in hardened concrete*. West Conshohocken, PA: ASTM International; 2021.

[25] British Standards Institution. *BS EN 12390-8:2019 Testing hardened concrete—Part 8: depth of penetration of water under pressure*. London: BSI; 2019.

[26] ASTM International. *ASTM C618-22 Standard specification for coal fly ash and raw or calcined natural pozzolan for use in concrete*. West Conshohocken, PA: ASTM International; 2022.

[27] Fernández-Jiménez A, Palomo A. Characterisation of fly ashes. Potential reactivity as alkaline cements. *Fuel*. 2003;82(18):2259–2265. https://doi.org/10.1016/S0016-2361(03)00194-7

[28] Duxson P, Provis JL, Lukey GC, Mallicoat SW, Kriven WM, van Deventer JSJ. Understanding the relationship between geopolymer composition, microstructure and mechanical properties. *Colloids Surf A*. 2005;269:47–58. https://doi.org/10.1016/j.colsurfa.2005.06.060

[29] He J, Jie Y, Zhang J, Yu Y, Zhang G. Synthesis and characterization of red mud and rice husk ash-based geopolymer composites. *Cem Concr Compos*. 2013;37:108–118. https://doi.org/10.1016/j.cemconcomp.2012.11.010

[30] Yip CK, Lukey GC, van Deventer JSJ. The coexistence of geopolymeric gel and calcium silicate hydrate at the early stage of alkaline activation. *Cem Concr Res*. 2005;35(9):1688–1697. https://doi.org/10.1016/j.cemconres.2004.10.042

[31] Nair DG, Fraaij A, Klaassen AAK, Kentgens APM. A structural investigation relating to the pozzolanic activity of rice husk ashes. *Cem Concr Res*. 2008;38:861–869. https://doi.org/10.1016/j.cemconres.2007.10.004

[32] Najafi Kani E, Allahverdi A, Provis JL. Efflorescence control in geopolymer binders based on natural pozzolan. *Cem Concr Compos*. 2012;34(1):25–33. https://doi.org/10.1016/j.cemconcomp.2011.07.007

[33] British Standards Institution. *BS 882:1992 Specification for aggregates from natural sources for concrete*. London: BSI; 1992.